RESEARCH PAPER

An experimental study of the performance of a finned tube solar collector on a single slope solar still

Hussein O. Abdulridha*, Hassanain G. Hameed, Basil N. Merzah

Engineering Technical College Al-Najaf, Al-Furat Al-Awsat Technical University, Al-Najaf, Iraq

Abstract

Water that can be consumed is necessary for life to exist. One of the biggest issues that humanity faces globally is access to drinking water, particularly in rural and dry areas. Solar distillation is now the most effective nonconventional and environmentally benign way to filter brackish or marine waters. This experimental work seeks to increase the yield of traditional single-slope solar stills using finned tube solar collectors. Experimental results carried out under the climatic conditions of Najaf, Iraq (32° 1 38.55″ N/44° 19′ 59.22′ ′E) showed that the maximum basin water temperature of finned tubes solar collector [modify solar still (MSS)] is 64.1 °C and for conventional solar still (CSS) is 45.8 °C at 14:00 p.m. This behavior is the same for the other temperatures (vapor, inner glass surface, and outer glass surface). Also, the water and inner glass surfaces' temperature difference (T_w-$T_{g,in}$) is 3.9 °C for MSS and 1.8 °C for CSS. The daily productivity of MSS is 4.766 l/m^2 day, with an enhancement of 65.12% as compared with that of CSS. The exergy efficiency increases with time to reach its maximum value of 32.53% at 15:00 p.m. for the MSS and 13.78% at 14:00 p.m. for the CSS. With respect to cost analysis, employing a finned tube collector alongside CSS affords the lowest cost per liter of distillate. Specifically, the cost is equivalent to 0.04 USD.

Keywords: Finned tubes, Fresh water, Solar collector, Solar distillation, Solar still

1. Introduction

The global community is currently facing a notable challenge regarding the accessibility of drinkable water, especially in distant and arid regions. In addition to sustenance and energy, the consumption of drinkable water is an imperative necessity for preserving life on our planet. Despite the fact that a substantial quantity of water is accessible, it is primarily brackish and unsuitable for utilization in farming, domestic applications, or industrial procedures.[1,2] Approximately 97% of the surface water on Earth appears as saline water in the seas and oceans. The minuscule residual fraction encompasses freshwater origins, including streams, reservoirs, and arctic reservoirs ensconced within glacial and polar ice formations.[3] In light of the prevailing circumstances, the utilization of solar energy in isolation for water distillation appears to hold great potential owing to its commendable attributes, namely the absence of carbon emissions, ecological compatibility, inexhaustible replenishment, and widespread availability.[4]

Due to its cost-effectiveness, ease of production, availability of raw materials, and user-friendly nature, conventional solar still (CSS) is the most prevalent variety. The scholars focused on enhancing the fundamental procedures that are imperative to the functioning of this system owing to its low yield, exemplified by the condensation procedure[5,6] or improving the evaporation process[7,8] or both.[9,10]

According to Sharshir et al.[11] thermal characteristics in untreated water are enhanced by incorporating nanoparticles, specifically copper oxide microflakes and graphite. The analysis of the results indicates that the utilization of copper oxide nanoparticles resulted in a notable 44.9% amplification in output, while the implementation of graphite

Received 8 August 2023; revised 23 December 2023; accepted 17 January 2024.
Available online 8 April 2024

* Corresponding author at: Engineering Technical College Al-Najaf, Al-Furat Al-Awsat Technical University, Al-Najaf, 31001, Iraq.
E-mail address: hussain.ms.etcn7@student.atu.edu.iq (H.O. Abdulridha).

https://doi.org/10.62593/2090-2468.1010

microflakes led to an even more significant productivity surge of 53.9%. Jaafar et al.[12] studied the improvement of the evaporation process for a single slope solar still (SSSS) by using a solar collecting tank to heat the water before entering the SSSS. It was found through conducting experiments that the improvement in yield was achieved by 48.83% by using this method. Zahraa Abdul Kareem et al.[13] investigate the use of custom-designed evacuated copper pipes with different diameters and water filling ratios to enhance the evaporation and thermal performance of a SSSS. Increasing the absorption of the solar still basin plate or enhancing the heat transfer with raw water can increase the production rates of pure water. Experimental investigations show that using evacuated pipes with a 15 mm diameter and a 50% filling ratio significantly improves the evaporation and thermal performance of the solar still, leading to a 90.09% increase in pure water productivity. The results suggest that the use of evacuated pipes can significantly impact the productivity of solar stills, and increasing the diameter of the pipes further enhances the performance. Hawraa et al.[14] study focuses on the numerical simulation of a heat exchanger within a single solar still containing PTC. The optimal design for the singular solar distillation apparatus was determined through a simulation conducted using the COMSOL 5.5 software. The simulation encompassed a heat exchanger design comprising a coiled and an evaporator (pipes mounted on the plate) type. One of the intended outcomes is to enhance productivity. Utilizing a heat exchanger located within a second type of solar still apparatus results in elevated temperatures from the coiled heat exchanger. Compared to the first type of heat exchanger, employment of the second type produces a greater yield of distilled water, attaining a rate of 5.35017 kg/m^{2}h over diurnal periods. Hameed[15] and Ghani et al.[16] presented a numerical analysis to examine the augmentation of the productivity of a single-slope, single-basin solar still through the creation of a novel absorbent base design aimed at increasing the evaporation surface area. The absorbent base design utilizes stainless steel geometries of varying shapes and sizes to accentuate their impact on solar still productivity. Findings indicate that using stainless steel geometries leads to an increase in evaporation rate and a consequent improvement in still productivity. The CSS productivity rate was calculated to be 2.987 kg/m^2, with maximum temperatures of still water and the inner surface of the glass cover measuring 63.6 and 54.2 °C, respectively. The highest freshwater productivity was achieved through the utilization of cones, with a resultant produced water rate of 4.13 kg/m^2 and an enhancement ratio of 38.2%. In this instance, the maximum temperatures of still water and the inner surface of the glass cover were recorded at 72.9 and 61.9 °C, respectively. Hameed[15] studied experimentally the evaluation of a SSSS with a square cross-section hollow fin attached to an absorber plate. The aim of the study is to find a more cost-effective solution for producing fresh water from salty water by using solar energy. The study also estimates the potential of cooling the glass cover. The results show that the solar's productivity was still enhanced by 40% by integrating it with fins and by 13.3–36.7% by integrating it with glass cooling by spraying at different rates. The combination of both mechanisms resulted in a further enhancement of 61.3% in contrast to that of a conventional SSSS. Abdullah et al.[17] experimentally investigated the performance of a modified solar still (MSS) and a CSS. The MSS had a copper water heating coil, internal reflector, external reflectors, nano-phase change material (PCM-Ag), and an external condenser. Five experiments were performed in the same climate to compare the performance of MSS and CSS. The use of the MSS-R, MSS-R-EC, MSS-R-PCM, and MSS (heating coil) resulted in a rise in productivity/thermal efficiency of 76/45.4, 134/54.1, 191/62, and 175%/60.2%, respectively. Integrating external reflectors (top and bottom) increased the productivity of MSS with internal reflectors by about 42%. Furthermore, using an external condenser improved MSS-R production by ~57% compared to the situation without one. Finally, the utilization of PCM boosted MSS-R productivity by ~41% over the case without PCM. Ramzy et al.[18] performed a study to improve the performance and productivity of solar stills by developing two stills with different natural and artificial absorbing materials, including black luffa, luffa, fine steel wool, and steel wool pads. The results showed that the selection of the absorbing material significantly impacted solar still productivity, with steel wool pads achieving the highest yield of 4.384 l/m^2. Furthermore, steel wool pads also exhibited the highest thermal efficiency at 32.74%.

In this paper, an experimental investigation on a finned tube solar collector incorporated with a SSSS was carried out. This work was adopted as a result of the severe lack, according to our limited vision, of the performance of the SSSS integrated with the finned collector in the atmosphere of Iraq. The results were compared CSS to determine the extent of improvement this system would show when combined with a CSS. The experiments were conducted under the climatic conditions of Najaf, Iraq, from February 5–25, 2023 (32° 1 38.55″ N/44° 19′ 59.22′ ′E).

1.1. Experimental work

The current study has constructed two indistinguishable prototypes of a SSSS. One is employed as a CSS for comparison, whereas the second prototype has been enhanced with a solar collector comprising finned tubes to increase the evaporation process within the still. This prototype is referred to as the MSS, as illustrated in Fig. 1.

The construction of CSS and MSS bodies has been carried out by employing two rectangular boxes made of polystyrene material. It is worth noting that polystyrene material exhibits a thermal conductivity of 0.03 W/m.K,[19] which qualifies it as a highly effective insulator. Consequently, insulating the sides and bottom of the stills is unnecessary. To ensure precision, a CNC machine has been utilized to cut the upper portion of the two boxes at an angle of 32° relative to the horizon, resulting in refined surfaces and edges. Each of the two stills possesses an area of 0.04 m^2, with the front and back sides having heights of 9 and 40 cm, respectively. The thickness of the sides of the employed boxes measures 4.5 cm.

A conventional glass sheet measuring 58.5 × 78 cm and having a thickness of 4 mm is positioned atop the still as a glass cover, allowing for the transmission of solar radiation at a transmittance percentage of 0.88. To prevent any potential leakage, a rubber sealing tape is inserted between the glass cover and the edges of the box. To collect any accumulated water, a water collecting channel, measuring 5 mm in width and inclined at an angle of 2°, has been excavated along the lower (front) side of the still. The water that accumulates in the channel then flows into a graduated flask with a capacity of 1 l. As an absorption unit, a galvanized sheet coated in matte black color for enhanced solar absorption has been affixed within the still basin. This galvanized sheet has a thickness of 2 mm and dimensions of 50 × 78 cm.

A solar collector was fabricated utilizing finned tubes, which possessed a diameter of 6 mm and a thickness of 0.6 mm. These tubes were affixed onto a galvanized plate, measuring 2 mm in thickness and having dimensions of 70.5 × 89 cm. Both the finned tubes and plate were coated with matte black paint to enhance the absorption of solar radiation. Furthermore, the compound was introduced into a wooden box, as depicted in Fig. 2.

The diagrammatic representation of CSS and MSS, as illustrated in Fig. 1, displays a solar collector inclined at an angle of 32°. This inclination allows for a higher solar gain during the peak time. Both stills and the collector are oriented towards the south, and all the experiments were conducted at the Engineering Technical College, Najaf, Iraq, from the February 10–25, 2023, between 8:00 a.m. and 17:00 p.m.

Temperatures are hourly assessed employing calibrated K-type thermocouples across solar stills and collectors (basin, water, vapor, inlet and outlet glass cover surfaces and inlet and outlet of collector). Seven thermocouples are utilized for CSS and 10 for MSS. Additionally, an extra thermocouple is employed for measuring ambient temperature. All thermocouples are connected to a digital data logger (AT4532), as depicted in Fig. 3a. The SM206 m (Fig. 3b) is employed to gauge the solar radiation every hour, with a range of 0–1370 W/m^2. The solar meter is inclined similarly to the glass cover to ensure precise radiation readings. Wind speed is observed each hour with a GM-8902 anemometer (Fig. 3c), with a reading range of 0–89 m/s. The

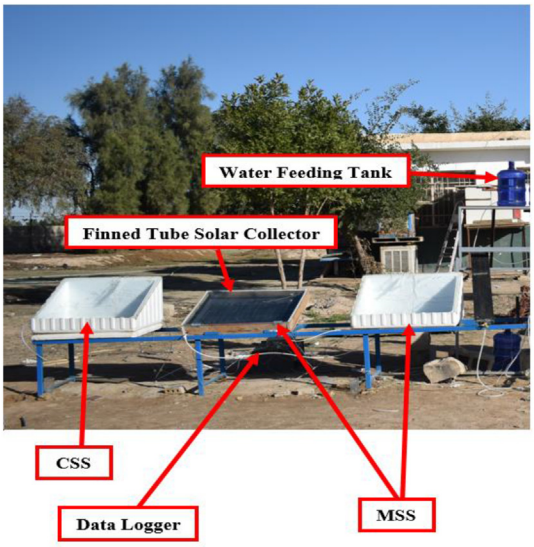

Fig. 1. Front view of CSS and MSS. CSS, conventional solar still; MSS, modify solar still.

Fig. 2. Pictorial view finned tube solar collector.

Fig. 3. (a) Digital data logger, (b) SM206 solar power meter, and (c) anemometer device (GM8902).

hourly yield is ascertained using a 1-l graduated flask.

Fig. 4 (a and b) and Table 1 display thermocouple installation sites for solar distiller and collector. Table 2 lists the range and accuracy. The standard uncertainties are obtained by considering linear data variation from equipment. Thus it is taken as $a/\sqrt{3}$ where a is the device accuracy.[20]

Table 2. Uncertainty and accuracy of the measuring devices.

Devices	Accuracy	Range	Standard uncertainty
Thermocouple	±1.2 °C	0–270 °C	0.692 °C
Solar power meter	±10 W/m^2	0–1370 W/m^2	5.77 W/m^2
Anemometer	±0.2 m/s	0–89 m/s	0.115 m/s
Flask water	±5 ml	0–1 l	2.88 ml

2. Experimental procedure

The solar devices for distillation and the apparatus for collection were oriented in a southerly direction, with the covers and collector positioned at an inclination of 32° to ensure optimal reception of solar radiation. As the radiation permeates the covers and reaches the foundation (where the absorption process occurs), it will induce a rise in

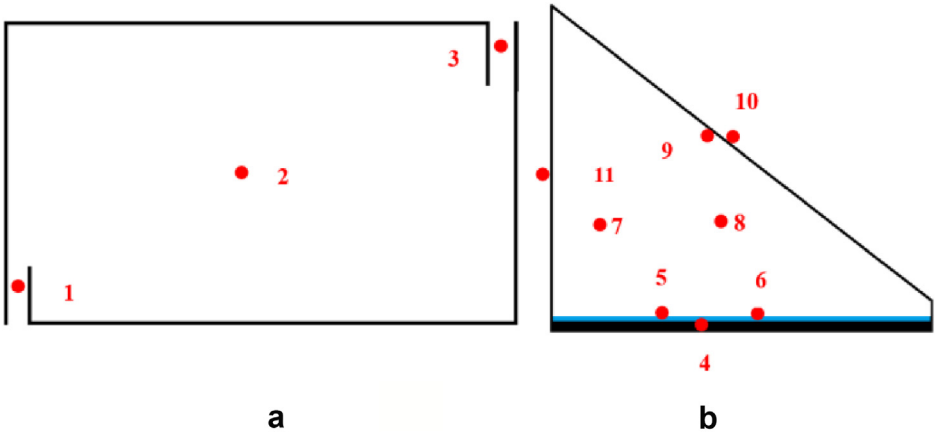

Fig. 4. Thermocouples locations for: (a) solar collector and (b) solar still.

Table 1. Thermocouples locations names.

Thermocouple no.	1	2	3	4	5, 6	7, 8	9, 10	11
Location	Inlet of collector	Collector plate surface (inside the cavity)	Outlet of collector	Galvanized plate	Basin water	Most air (vapor zone)	Inner and outer glass surfaces	Ambient (on the back side of the still)

temperature, subsequently elevating the water temperature above the foundation. The water level, which has been carefully maintained at 0.5 cm, is considered to be the optimal level for achieving maximum productivity in the distillation process.[21,22] The total dissolved solids of the water utilized in these experiments fall within the range of 2700–4000 parts per million. Once the water temperature surpasses a specific threshold and by the prevailing conditions, it will commence the process of upward evaporation, coming into contact with the inclined glass surface, characterized by a lower temperature. This interaction results in vapor condensation on the cover's inner surface, manifesting as droplets. Subsequently, these droplets descend downward due to the inclination of the cover towards the collection channel, facilitating the transfer of the resulting yield to the flask.

3. Exergy analysis of solar still

The exergy analysis of the still is conducted by utilizing the governing equations established upon the principles of the second law of thermodynamics. Consequently, the general form of the exergy balance can be articulated as described in the subsequent manner.[23]

$$E_{x,dest} = E_{x,in} + E_{x,out} \tag{1}$$

$$E_{x,in} = E_{x,sun} = I_t A_b \left[1 + \frac{4}{3}\left(\frac{T_{amb}+273.16}{T_{sun}}\right) - \frac{1}{3}\left(\frac{T_{amb}+273.16}{T_{sun}}\right)^4\right] \tag{2}$$

$$E_{x,out} = E_{x,evap} = \frac{m_{evap}\, h_{fg}}{3600}\left[1 - \left(\frac{T_{amb}+273.16}{T_w+273.16}\right)\right] \tag{3}$$

$$h_{fg} = 2.4935*10^6 * \left(1 - 9.4779*10^{-4}*T_{w,b} + 1.3132*10^{-7}*T_{w,b}^2 - 4.7974*10^{-9}*T_{w,b}^3\right. \tag{4}$$

where I_t is the solar radiation incident on the still, A_b is the basin area, and T_{sun} is the sun's temperature, taken as 6000 K. h_{fg} is latent heat of vaporization. m_{evap} is amount of water evaporation. T_w is temperature of water. The exergy efficiency is thus calculated as the proportion of the still's output to its input, which can be expressed as follows.[23]

$$\eta_{EX} = \frac{E_{x,out}}{E_{x,in}} = \frac{E_{x,evap}}{E_{x,sun}} \tag{5}$$

4. Results and discussion

Fig. 5 shows the behavior of wind speed, solar radiation, and air temperature during one of the experiment's test days. It is clear from the figure that the parameters increase with time to reach its maximum value between 12:00 and 14:00 p.m., and the decrease with time progress.

Figs. 6 and 7 show the temperature behavior of basin water, vapor, inner and outer glass cover surface with time for CSS and MSS. All temperatures increase over time to achieve the highest value at 14:00 p.m., then gradually decrease to its lowest value. This behavior is consistent with the behavior of solar radiation throughout the experiment. It is also clear from the figures that the MSS have temperatures higher than the CSS due to the presence of solar collectors.

Fig. 8 shows the temperature difference of the water (Tout–Tin) passing through the solar collector and entering the still along the experiment time. From the figure it can be noticed that the temperature difference increased to maximum value of 43.1 °C, and then decreased as the behavior of solar radiation. Through the figure, it is noted that the temperature of the water entering the distillation apparatus has a clear effect in reducing the evaporation time of the water.

Fig. 9 shows the difference in temperature between the basin water (Tw) and inner glass surface (Tg, in) (Tw-Tg, in) over the time of the experiment. It is clear from the figure that the MSS operate with a temperature difference higher than the CSS, which gives preference to MSS in performance and increased productivity. The most important factor that indicates the amount of still yield increase is the difference temperature between the basin water and inner glass cover. Whereas the increase in this difference leads to an increase in the still outcome due to the enhancement of the condensation process inside the still.

Fig. 10 shows the total productivity of the CSS and MSS during the day of the experiment. It is evident from the figure that the preference in productivity belongs to the MSS due to the presence of the solar collector. Whereas it is 4.766 l/m^2/day for MSS and 2.886 l/m^2/day for CSS.

Fig. 11 shows the behavior of exergy efficiency during one of the test days of the experiment. It is clear from the figure that the exergy efficiency increases with time to reach its maximum value of 32.53% at 15:00 p.m. for the MSS and 13.78% at 14:00 p.m. for the CSS.

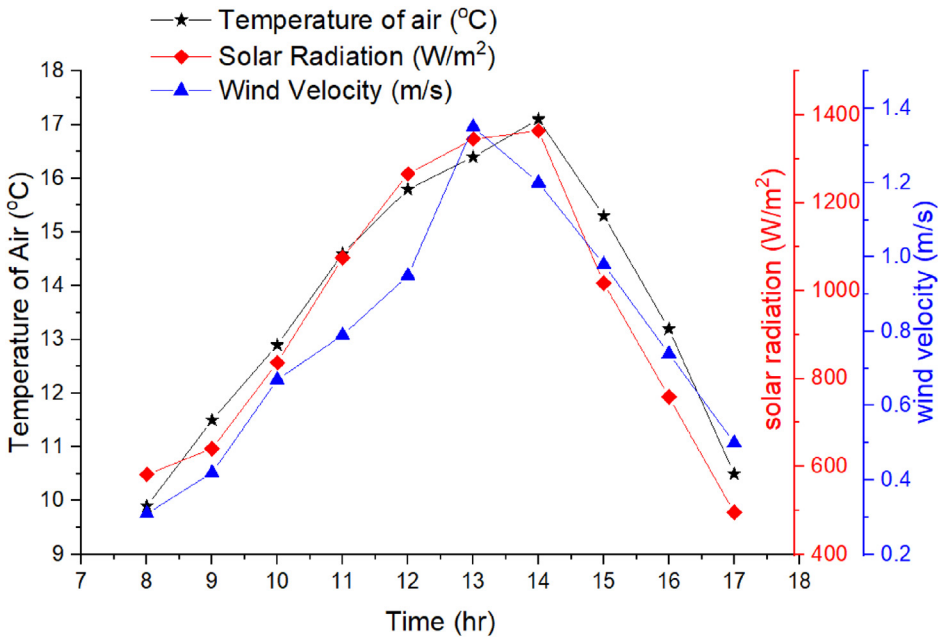

Fig. 5. Variation of wind velocity, solar radiation and temperature of air with the time of experiment on 9/2/2023.

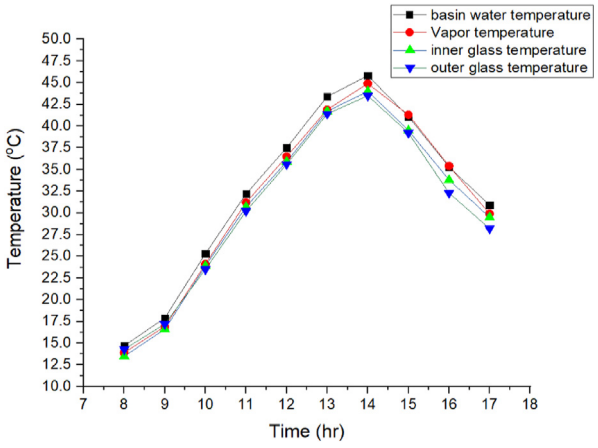

Fig. 6. Variation of the temperature of basin water, vapor, inner and outer glass cover surface with time for CSS in 9/2/2023. CSS, conventional solar still.

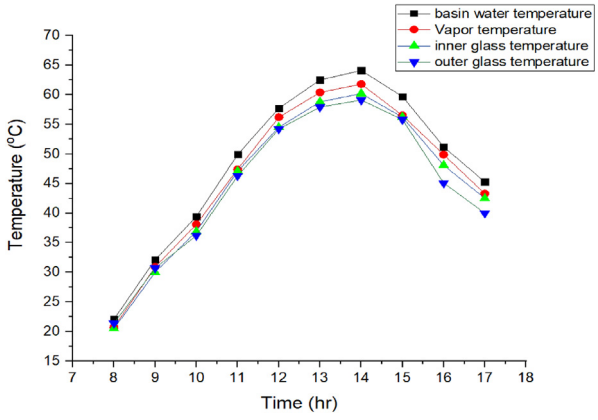

Fig. 7. Variation of the temperature of basin water, vapor, inner and outer glass cover surface with time for MSS in 9/2/2023. MSS, modify solar still.

4.1. Cost analysis for stills

The type of solar still and its components with all its accessories are the basic requirements in the cost analysis calculations. So, cost estimation is performed for both variable and fixed costs. Table 3 lists the components and its cost for the two stills. Depending on the still lifetime and the daily yield, the cost of 1 l from the still can be determined as follows:[24]

$$C\,(\text{the annual total cost}) = F\,(\text{fixed cost}) + V\,(\text{variable cost}) \quad (6)$$

The following requirements can be considered to facilitate and achieve the cost calculation process.[25]

(1) The lifetime of the still is 5 years.
(2) The solar still operates for 325 days in a year.
(3) Variable cost (V) is equal to 0.3 fixed cost (F) per year, including the maintenance cost.

4.2. Conventional solar still

The fixed cost of CSS is $F = 85.25$ \$ per 1 m^2, thus, from equation (1).

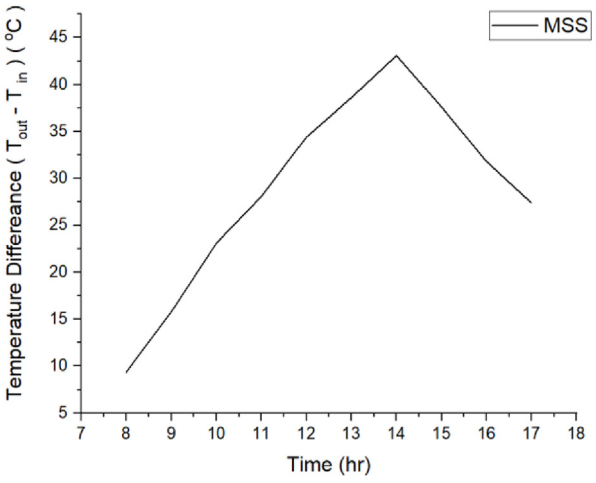

Fig. 8. Temperature difference and time (Tout−Tin) for MSS in 9/2/2023. MSS, modify solar still.

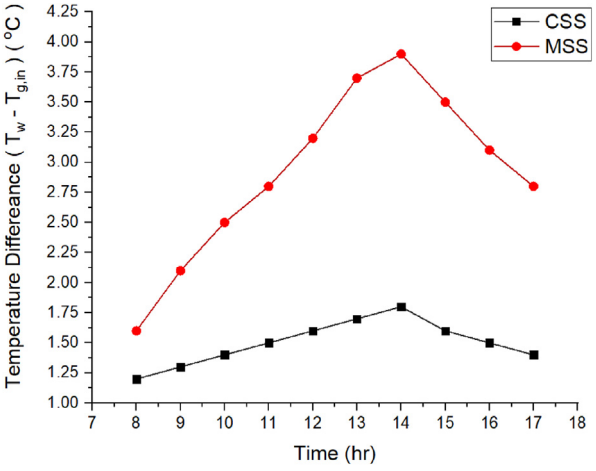

Fig. 9. Temperature difference along with time (Tw−Tg, in) for CSS and MSS on 9/2/2023. CSS, conventional solar still; MSS, modify solar still.

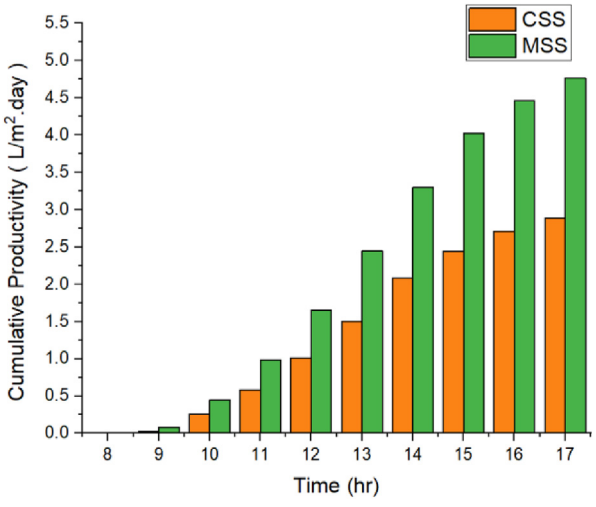

Fig. 10. Cumulative productivity for CSS and MSS. CSS, conventional solar still; MSS, modify solar still.

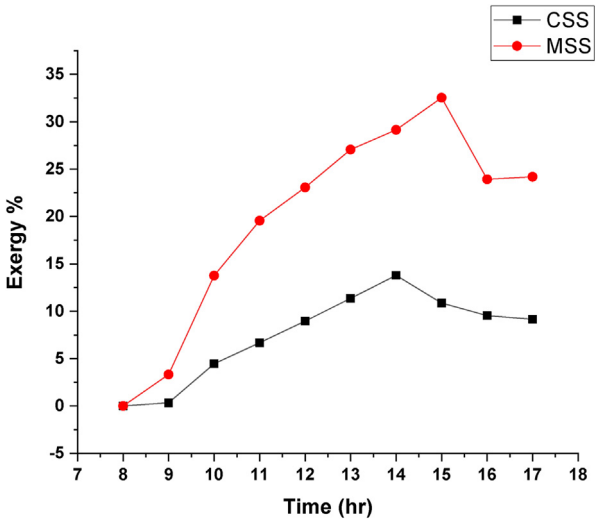

Fig. 11. Exergy efficiency for CSS and MSS. CSS, conventional solar still; MSS, modify solar still.

Table 3. Cost of the two fabricated still models.

Items	Cost ($)	
	MSS	CSS
Polystyrene box	26.25	26.25
CNC shaping of box	7.5	7.5
Galvanized iron sheet	34	25
Paint	13	7.5
Glass cover	16	10
Plastic pipe	2	1
Flexible rubber band	6.5	4
Auxiliaries (silicon, tab, etc.)	5	4
Finned tubes	9	/
Wood	6	/
Total fixed cost of SSSS with an absorbing area of 1 m^2	125.25	85.25

CSS, conventional solar still; MSS, modify solar still.

C = 85.25+(0.3 × 85.25 × 5) = 213.125 $. The average daily productivity of CSS is about 2.886 l/m^2. Then, the production during the life of still is 2.886 × 325 × 5 = 4689.75 l.

Thus, the cost of 1 l from CSS = 213.125/4689.75 = 0.045 $.

4.3. Modify solar still

The fixed cost of CSS is $F = 129.25$ $ per 1 m^2, thus, from equation (1).

C = 125.25+(0.3 × 125.25 × 5) = 313.125 $. The average daily productivity of CSS with finned tubes collectors is about 4.766 l/m^2. Then, the production during the life of the still is 4.766 × 325 × 5 = 7744.75 l.

Thus, the cost of 1 l from CSS-finned tube collector-solar still technology = 313.125/7744.75 = 0.04 $.

Table 4. Compression of the current study with other studies.

References	Date/country	Adopted technique	% enhancement in productivity	Productivity ($l/m^2.day$)	Cost $
Alwan et al.[26]	2020/Iraq	Hollow cylinder that slowly rotates within a solar water unit and integrated with outer solar collector	292%	5.5	0.048
Rajaseenivasan et al.[27]	2014/India	Using flat plat collector	60%	5.82	0.037
Kumar et al.[28]	2020/India	Using flat plat collector	57.07%	1.59	–
Jaafar et al.[12]	2020/Iraq	Solar collecting tank compared with conventional solar still	48.83%	2.1	0.052
Current study	February 2023/Iraq	Using finned tubes solar collectors	65.12%	4.766	0.04

The comparison of the SSSS performance of previous related authors works, and the present is depicted in Table 4.

4.4. Conclusions

This work investigates the performance of two models of SSSS. The two models are CSS and MSS. The MSS is considered as CSS integrated with a finned tube solar collector.

Under the environmental conditions, the experimental results showed that the use of finned tube collector-solar still technology results in a noteworthy increase in basin water temperature up to a maximum of 64.1 °C during peak intervals, surpassing the 45.8 °C utilizing CSS, thereby suggesting its potential for efficient thermal energy conversion.

This phenomenon results in a beneficial effect on the remaining thermal conditions within the still, consequently reducing the duration of water evaporation in the still basin and enhancing operational efficiency. Implementing finned tubes has significantly increased the aggregate daily output of solar systems by as much as 65.12%. The finned tube collector-solar still technology under study operates at a Tout–Tin temperature of 3.9 °C. Furthermore, according to the cost analysis, the cost of producing 1 l of pure water using CSS was 0.045 USD, and reduced by 11.11% when using the MSS.

Author contributions

Hussein Oleiwi Abdulridha: Installing the experimental parts, recording the readings, extracting the results, writing the research paper initially, and taking pictures. **Hassanain Ghani Hameed:** Developing the research plan, designing the experimental parts, reviewing and revising the writing of the research paper, checking the results, verifying the references, and supervising the experiments. **Basil N. Merzah:** Installing the experimental parts, reviewing the results, verifying the references, and supervising the experiments.

Funding

The entire work of this article is funded by the authors and there is no governmental or community funder.

Conflict of interest

The authors declare that they have no known competing financial interests or personal relationships that could have appeared to influence the work reported in this paper.

References

1. Yousef MS, Hassan H, Ahmed M, Ookawara S. Energy and exergy analysis of single slope passive solar still under Egyptian climate conditions. *Energy Proc*. 2017;141:18–23.
2. Elbar ARA, Hassan H, Ookawara S. A numerical study on the effect of the heat sink as condenser on the performance of passive solar still. In: *5th Int Conf Renew Energy Gener Appl 2018*. 2018:256–259.
3. Fathy M, Hassan H, Salem Ahmed M. Experimental study on the effect of coupling parabolic trough collector with double slope solar still on its performance. *Sol Energy*. 2018;163:54–61.
4. Chaichan MT, Kazem HA. Water solar distiller productivity enhancement using concentrating solar water heater and phase change material (PCM). *Case Stud Therm Eng*. 2015;5:151–159.
5. Kabeel AE, Omara ZM, Essa FA. Enhancement of modified solar still integrated with external condenser using nanofluids: an experimental approach. *Energy Convers Manag*. 2014;78:493–498.
6. Zanganeh P, Goharrizi AS, Ayatollahi S, Feilizadeh M. Nano-coated condensation surfaces enhanced the productivity of the single-slope solar still by changing the condensation mechanism. *J Clean Prod*. 2020;265:121758.
7. Ramanathan V, Kanimozhi B, Bhojwani VK. Experimental study on productivity of modified single-basin solar still with a flat plate absorber. *IOP Conf Ser Mater Sci Eng*. 2017;197:1.
8. Dumka P, Kushwah Y, Sharma A, Mishra DR. Comparative analysis and experimental evaluation of single slope solar still augmented with permanent magnets and conventional solar still. *Desalination*. 2019;459:34–45.
9. Bhargva M, Yadav A. Effect of shading and evaporative cooling of glass cover on the performance of evacuated tube-augmented solar still. *Environ Dev Sustain*. 2020;22:4125–4143.

10. Suraparaju SK. Combined enhancement of evaporation and condensation rates in the solar still for augmenting the freshwater productivity using energy storage and natural fibres. *Water Infrastruct Ecosyst Soc*. 2022;71:628–641.
11. Mohamed SIT, Kabeel AE. Enhancing the solar still performance using nanofluids and glass cover cooling : experimental study state key laboratory of coal combustion , Huazhong university of science and technology , nano interface center for energy (NICE), school of energy and P. *Appl Therm Eng*. 2016;113:1.
12. Jaafar ZA, Hameed HG, Hussein RH. Experimental investigation of a single slope solar still performance – evaporation process enhancement. *IOP Conf Ser Mater Sci Eng*. 2020;928:2.
13. Jaafar ZA, Hameed HG. Experimental investigation of a single slope solar still performance-evaporation process enhancement using evacuated pipes. *IOP Conf Ser Earth Environ Sci*. 2021;877:1.
14. Fadhel H, Abed QA, Hachim DM. Numerical simulation of heat exchanger inside the single solar still with PTC. *AIP Conf Proc*. 12 April 2023;2776(1):050009. https://doi.org/10.1063/5.0136232.
15. Hameed HG. Experimentally evaluating the performance of single slope solar still with glass cover cooling and square cross-section hollow fins. *Case Stud Therm Eng*. 2022;40:102547.
16. Ghani H, Azeez H, Diabil N, Al-moussawi MA. A numerical investigation of the enhancement of single-slope single-basin solar still productivity. *Energy Rep*. 2022;9:484–500.
17. Abdullah AS, Alawee WH, Mohammed SA, Majdi A, Omara ZM, Younes MM. Utilizing a single slope solar still with copper heating coil, external condenser, phase change material, along with internal and external reflectors – experimental study. *J Energy Storage*. 2023;63:106899.
18. Ramzy K, Abdelgaleel M, Elnaby A, Mosalam H. Performance of a single slope solar still using different porous absorbing materials : an experimental approach. *Environ Sci Pollut Res*. 2023;30:72398–72414.
19. Ali Saeed MM, Hachim DM, Hameed HG. Numerical investigation for single slope solar still performance with optimal amount of Nano-PCM. *J Adv Res Fluid Mech Therm Sci*. 2019;63:302–316.
20. Dumka P, Mishra DR. Performance evaluation of single slope solar still augmented with the ultrasonic fogger. *Energy*. 2020;190:116398.
21. Al Shabibi AM, Tahat M. Thermal performance of a single slope solar water still with enhanced solar heating system. *Renew Energy Power Qual J*. 2015;1:585–587.
22. Aljubouri AA. Design and manufacturing of single sloped solar still: study the effect of inclination angle and water depth on still performance. *J Al-Nahrain Univ*. 2017;20:60–70.
23. Khafaji HQA, Wahhab HAA, Al-Maliki WAK, Alobaid F, Epple B. Energy and exergy analysis for single slope passive solar still with different water depth located in Baghdad center. *Appl Sci*. 2022;12:050009. https://doi.org/10.1063/5.0136232.
24. Abdullah AS, Omara ZM, Alarjani A, Essa FA. Experimental investigation of a new design of drum solar still with reflectors under different conditions. *Case Stud Therm Eng*. 2021;24:100850.
25. Eltawil MA, Omara ZM. Enhancing the solar still performance using solar photovoltaic, flat plate collector and hot air. *Desalination*. 2014;349:1–9.
26. Alwan NT, Shcheklein SE, Ali OM. Experimental investigation of modified solar still integrated with solar collector. *Case Stud Therm Eng*. 2020;19:100614.
27. Rajaseenivasan T, Nelson Raja P, Srithar K. An experimental investigation on a solar still with an integrated flat plate collector. *Desalination*. 2014;347:131–137.
28. Kumar D, Layek A, Kumar A. Performance enhancement of single slope solar still integrated with flat plate collector for different basin water depth. *AIP Conf Proc*. 2020;2273:50007.